

## Random Polybutadiene Rubber Networks with Unattached Chains

Sokol Ndoni,<sup>\*,†</sup> Allan Vorup,<sup>‡</sup> and Ole Kramer<sup>‡</sup>

Condensed Matter Physics and Chemistry Department, Risoe National Laboratory, P.O. Box 49, DK-4000 Roskilde, Denmark, and Department of Chemistry, University of Copenhagen, Symbion, Fruebjergvej 3, DK-2100 Copenhagen, Denmark

Received September 25, 1997; Revised Manuscript Received December 26, 1997

**ABSTRACT:** The preparation and characterization of *randomly cross-linked polybutadiene (PB) networks containing unattached PB chains* are presented. These were used as model systems for the experimental study of the dynamics of linear chains trapped in networks, which is the basic model of the reptation-in-a-tube model of Doi and Edwards. The preparation consists of the conversion at random of a small fraction of the PB chains' double bonds into epoxide groups and in the subsequent selective use of these as cross-linking centers in the presence of unmodified PB chains; these last remain chemically unattached to the network. The selectivity of the cross-linking reaction was examined by swelling–extraction of networks containing known fractions of relatively short “monodisperse” unattached chains. The polymeric phase composition of the networks with unattached chains (*nuc*) was tested by glass transition temperature measurements. Dynamic–mechanical measurements were shown to be sensitive to the polymer-phase composition of *nuc*, as well. The dynamics of the linear PB chains in the melts and in the networks was studied by dynamic–mechanical measurements. The experimental results for the longest relaxation time  $\tau_L$  were compared with the predictions of the reptation-in-a-tube model with and without chain-end effects. Within experimental accuracy, the obtained scaling of  $\tau_L$  relative to the chain mass  $M$  (up to  $9 \times 10^5$  g/mol) is the same in both media:  $\tau_L \sim M^x$  with  $x = 3.35 (\pm 0.10)$  as against  $x = \pm 3$  from the pure reptation-in-a-tube model; correcting for chain-end effects in the form of contour length fluctuation, results in a good description of the experimental data for the  $\tau_L$ s of unattached chains.  $\tau_L$  for the chains trapped in networks were found to be 1.9–3.2 times longer than the  $\tau_L$  of the respective melts. Data on 14 PB prepared by anionic polymerization and covering the range of weight average molar masses  $1.0 \times 10^4$  to  $1.5 \times 10^6$  g/mol are presented.

## Introduction

Rubber networks with unattached chains<sup>1–7</sup> are ideally one-phase, two-component systems; the first component is one macroscopic molecule (the network) and the second consists of linear chains “dissolved” into the network. The materials (with or without phase separation) are also classified in the literature as “semi-interpenetrating networks” (sIPN).<sup>8</sup>

Because the short time dynamics (glass and transition regions<sup>1</sup>) of a rubber network is essentially the same as that of a high polymer melt,<sup>1</sup> the rubber networks containing small concentrations of unattached chains permit one to study the dynamics of almost isolated chains in the rubber plateau and the terminal zones.<sup>1</sup> Therefore, these systems can be used to test the predictions of one-chain theoretical models (specifically the reptation-in-a-tube model<sup>9–12</sup>) and as references for the study of polymer melts. On the other hand, the same systems are well-fitted for the investigation of the long-time (eventually equilibrium) properties of rubber networks as depending on the degree of cross-linking. The analysis of the contribution from the unattached chains to the loss modulus in dynamic–mechanical tests<sup>1</sup> becomes straightforward when the relaxation from the network component is comparatively small in the interesting time-scale range. This is shown to be the case for the networks with a low content of long unattached chains from the present work. From the material point of view, the networks with unattached chains (*nuc*) combine the permanency of covalent networks with the properties of polymer melts.

The first elastomeric *nuc* were prepared by the group of Ferry at Wisconsin.<sup>2–6</sup> The present work extends the class of *nuc* with the *random networks of polybutadiene (PB) homopolymer*.<sup>13–16</sup> The procedure described below might be readily applicable to other polydiene elastomers. It consists of the random epoxidation of PB, the fraction of the epoxidized double bonds being in the range 0.03–0.04, followed by the *selective* use of the epoxide groups as cross-linking centers. Because of this selectivity and of the opportunity to synthesize PB with very narrow distribution of molar masses by living anionic polymerization,<sup>17–19</sup> we succeeded in preparing well-characterized *model systems*.

Why are the PB networks with PB unattached chains and the procedures presented here interesting and how do they compare with the previous literature reports<sup>2–7</sup> (only the rubber networks (no solvent) are considered)? The following answer relates only to the aspect of the use of *nuc* for testing the single-chain long-time dynamics. The materials and procedures presented in this contribution combine the following *advantages*: (1) almost constant storage moduli for the networks with 0% unattached chains in the rubber zone<sup>1</sup> that extends virtually to infinite time; (2) essentially the same time–temperature (for 200 K <  $T$  < 300 K) behavior<sup>1</sup> for both the network and the unattached components; (3) one of the lowest characteristic molar masses between the entanglements;<sup>1</sup> (4) samples with very narrow molar mass distributions; (5) high selectivity of the cross-linking reaction; (6) miscibility at the molecular level between the components for low concentration of the unattached component in a wide range of chain lengths; (7) because of the points 1, 2, and 4–6, accurate

<sup>†</sup> Risoe National Laboratory.

<sup>‡</sup> University of Copenhagen.

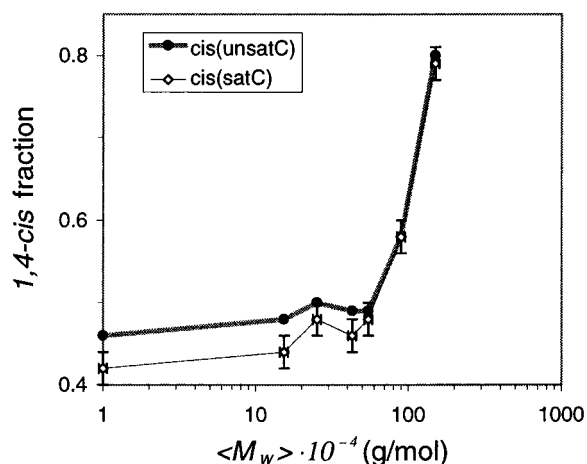


**Figure 1.**  $^{13}\text{C}$  NMR results on the PB cis content as a function of  $\langle M_w \rangle$  (see also Table 1).

dynamic-mechanical measurements allow a straightforward analysis of the contribution from the unattached chains to the loss moduli of the nuc with relatively low concentrations (10–15%) of long unattached chains. There is no need to obtain the unattached component contribution to the relaxation as a difference between two large contributions (as is the case for the stress-relaxation experiments used in many of the previous studies<sup>2–6</sup>). The PB nuc set of this work is unique in satisfying properties 1–6 above.

There are though two intrinsic *drawbacks* related to PB: (I) The microstructure of PB synthesized by living anionic polymerization in a nonpolar solvent (cyclohexane in the present case) and with alkylolithium initiator,<sup>17–19</sup> depends on the molar mass<sup>18</sup> (see Figure 1); (II) at normal conditions the double bonds in PB are not very stable for longer periods (weeks), and even at about  $-20^\circ\text{C}$  it is possible to measure (after 2–3 years) changes in the materials, probably due to free radical cross-linking.

The remainder of the paper is organized as follows. The description of the origin or synthesis of the PB materials is found at the start of the Experimental Section. The procedures of epoxidation, cross-linking, and swelling are then described. The Experimental Section is concluded with a listing of the instrumental techniques used for the sample characterization (nuclear magnetic resonance (NMR), rheometry, and differential scanning calorimetry (DSC)). In Results and Discussion the characterization of the PBs are first presented (molar masses and their distributions, microstructures, and glass transition temperatures  $T_g$ ). Then some space is dedicated to the important issues of the selectivity of the cross-linking reaction and of the phase composition of the nuc. The results and discussion of the dynamic-mechanical measurements and the comparison of the experimental with the Doi-Edwards predicted dependencies of the longest relaxation time on the chain length are found at the final part of the section. Because this last issue has already been reported in a separate publication,<sup>14</sup> only the main results are summarized here. Some conclusions from the present contribution are found at the last section.

## Experimental Section

**Polymers.** Three groups of polybutadienes (PBs) were used: two commercial anionic PBs (BUNA CB HX 530 SIC and CB HX 503 SIC, Bayer), kindly offered by Codan Gummi

A/S, Denmark; eight “monodisperse” PB calibration standards for size exclusion chromatography (SEC) from the Polymer Laboratories Ltd., covering the range of molar masses between  $8.3 \times 10^3$  and  $9.5 \times 10^5$  g/mol. These were used for the calibration of SEC and four of them, with masses between  $1.9 \times 10^4$  and  $1.2 \times 10^5$  g/mol were used as unattached chains, as well; our own anionic polybutadienes (14 PB samples with weight average molar masses between  $9.9 \times 10^3$  and  $1.5 \times 10^6$  g/mol were prepared by the technique of living anionic polymerization under inert (argon) atmosphere).<sup>15,20</sup> The polymerizations were made in cyclohexane at  $37 \pm 1^\circ\text{C}$  with 15–30 g/L initial monomer concentrations. The initiator was *sec*-butyllithium (Aldrich; 1.2 M solution in cyclohexane/hexane), titrated by the Gilman procedure.<sup>21,22</sup> For the samples with number average molar masses above  $3 \times 10^5$  g/mol a 12 times diluted initiator solution in cyclohexane was used in order to have a better measure of the injected volume. The prepared PB masses and mass distributions were determined by SEC.<sup>15</sup> The weight average molar masses  $\langle M_w \rangle$  of five PB samples were determined by low-angle laser light scattering (LALLS) on a Chromatix KMX-6 instrument. The masses obtained by SEC were within 2–8% of the target masses for all but the sample with the highest mass ( $\langle M_w \rangle = 1.5 \times 10^6$  g/mol). For that sample the target number average molar mass was  $2 \times 10^6$  g/mol; the polymerization in that case was terminated after 36 h, and by that time the magnetic stirring was not possible because of the high viscosity of the solution. The PB samples were further characterized by NMR (microstructure) and rheometry.

**Epoxidation of PB.** Monoperoxyphthalic acid was used as the oxidizing agent in toluene.<sup>15,16,23</sup> The content of epoxide in the slightly epoxidized PB (ePB) was determined by titration of epoxide groups with 0.0200 M solutions of hydrogen bromide in glacial acetic acid<sup>24</sup> and by  $^1\text{H}$  and  $^{13}\text{C}$  NMR.<sup>15,25</sup>

**Cross-Linking of ePB.** The prepared ePBs were used to produce cross-linked networks by the reaction of the epoxide groups with phthalic anhydride (>98%, Merck) in the presence of *N,N*-dimethylbenzylamine (98%, Merck) as catalyst.<sup>26</sup> The molar ratios between epoxide groups in the ePB to anhydride to catalyst (*e:a:c*) were in the ranges 1:(0.35–0.5):(0.15–0.5). Antioxidant BHT (98%, Merck) was used for all of the networks (0.1–0.2% of the total polymer mass). The cross-linking reaction of toluene-cast films took place under argon atmosphere<sup>20</sup> at  $140 \pm 10^\circ\text{C}$  (2–5 h).<sup>15</sup>

The cross-linked samples were 0.6–1.5 mm thick films; disks of diameter 4–10 mm were cut from these films and used for rheological, swelling, and swelling-extraction characterization. Five networks, containing between 39.5 and 10.1% of two relatively low molar mass PBs as unattached chains, were prepared for the swelling-extraction experiments in benzene. Prefiltered benzene extractions were characterized by SEC.

**NMR.**  $^1\text{H}$  NMR and  $^{13}\text{C}$  NMR spectra of 2–5% solutions in toluene-*d* or in chloroform-*d* were obtained from two instruments: a 400 MHz Varian spectrometer and a 250 MHz Bruker spectrometer. The relaxation delays used for the  $^1\text{H}$  NMR and  $^{13}\text{C}$  NMR measurements were varied between 1 and 30 s with total acquisition times varying between 10 and 3000 min.<sup>25</sup>

**Rheometry.** The dynamic-mechanical measurements were made on three strain-controlled oscillatory rheometers: Bohlin VOR, Rheometrics RMS-800, and Rheometrics solid analyzer RSA II, at  $25 \pm 0.5$ ,  $-75 \pm 1$ ,  $-60 \pm 1$ ,  $-50 \pm 1$ ,  $-25 \pm 1$ ,  $-13 \pm 1$ , and  $0 \pm 0.5^\circ\text{C}$ . The following test geometries<sup>1</sup> were used: parallel plates, pp; cone and plate, cp (only for the melts), and simple elongation, se (only for the networks). Delay times of two or more oscillation periods were applied for the frequency range  $\omega = 3 \times 10^{-4}$  to  $10^2$  rad/s. The samples were cylinders with  $h \times d = (0.6\text{--}3 \text{ mm}) \times (4\text{--}10 \text{ mm})$  for cp, pp and sheets  $l \times b \times h = (40 \text{ mm}) \times (5\text{--}10 \text{ mm}) \times (0.6\text{--}1.5 \text{ mm})$  for se. The oscillatory deformations were below 5% (typically 0.2–2%), and the static deformations for pp and se were less than 10%.

**Thermal Analysis.** Some of the samples were characterized by differential scanning calorimetry (DSC) on a Perkin-

Table 1. Characteristics of 20 PB and 4 ePB Used in the Present Work

PB samples name	$\langle M_w \rangle \times 10^{-3}$ (SEC)	PDI (SEC)	cis/trans/vinyl (NMR)	$T_g^{(20K/min)}/K$ (DSC)	ePB samples name	% epox <sup>e</sup>
CBHX530 <sup>a</sup>	490	2.4	38/51/11	183	ePB 1	3.7 (4.0)
CBHX503 <sup>a</sup>	260	2.2	38/51/11	183	ePB 3	3.4 (3.8)
PB10	9.90	1.06	42 <sup>c</sup> (46 <sup>d</sup> )/52 <sup>c</sup> (48 <sup>d</sup> )/6	176		
PB19 <sup>a</sup>	18.6	1.03				
PB34 <sup>a</sup>	34.0	1.04		177		
PB50	50.0	1.04		177		
PB64	64.0	1.04				
PB81 <sup>a</sup>	80.6 <sup>a</sup>	1.03				
PB120 <sup>a</sup>	120 <sup>a</sup>	1.03				
PB154	154	1.04	44 <sup>c</sup> (48 <sup>d</sup> )/50 <sup>c</sup> (46 <sup>d</sup> )/6			
PB174	174	1.05				
PB235	235 <sup>b</sup> (190)	1.26		178		
PB253	253	1.04	48 <sup>c</sup> (50 <sup>d</sup> )/47 <sup>c</sup> (45 <sup>d</sup> )/5	179	ePB 2	3.6 (4.0)
PB263	263	1.04				
PB345	345	1.05				
PB430	430 <sup>b</sup> (380)	1.10	46 <sup>c</sup> (49 <sup>d</sup> )/48 <sup>c</sup> (45 <sup>d</sup> )/6	179		
PB550	550 <sup>b</sup> (530)	1.06	48 <sup>c</sup> (49 <sup>d</sup> )/47 <sup>c</sup> (46 <sup>d</sup> )/5			
PB700	700	1.23		176		
PB900	900 <sup>b</sup> (830)	1.07	58 <sup>c</sup> (58 <sup>d</sup> )/36 <sup>c</sup> (36 <sup>d</sup> )/6	176	ePB 4	3.0 (3.3)
PB1500	1500 <sup>b</sup>	1.34	79 <sup>c</sup> (80 <sup>d</sup> )/17 <sup>c</sup> (16 <sup>d</sup> )/4	175		

<sup>a</sup> Commercial samples with characteristics as given by the producers. <sup>b</sup>  $\langle M_w \rangle$  obtained by LALLS. <sup>c</sup> Saturated C. <sup>d</sup> Unsaturated C, in <sup>13</sup>C NMR; the vinyl content was determined by <sup>1</sup>H NMR. <sup>e</sup> Measured by titrimetry and NMR.

Elmer DSC-7 system, cooled with liquid nitrogen. The samples were cooled to  $-150^\circ\text{C}$  by  $-100^\circ\text{C}/\text{min}$ , and after equilibration at this temperature they were scanned at  $20^\circ\text{C}/\text{min}$ , up to  $-20^\circ\text{C}$ . A second cycle (same conditions) right after the first did not show noticeable differences in the respective thermograms.

## Results and Discussion

**PB Synthesis and Characterization.** The characteristics of 20 polybutadienes used in the present study are summarized in Table 1. In the estimations of the polydispersity indices given in the third column of Table 1, there was correction for the SEC peak broadening by taking as reference the peak of the antioxidant BHT. Five samples (with the superscript *b* in the second column) were characterized by LALLS, and the obtained values of  $\langle M_w \rangle$  are somewhat different from those obtained by SEC. The LALLS values of  $\langle M_w \rangle$  were taken as more appropriate for the respective samples.

The cis–trans content of five PB samples, as obtained from the integrals of the saturated and unsaturated parts of the <sup>13</sup>C NMR spectra, are given in Table 1 (fourth column) and in Figure 1. There is some variation between the cis (trans) fractions estimated by the two regions of the spectra, but the general trend is an increase in the cis content with increasing  $\langle M_w \rangle$ .<sup>18,27,28</sup> It is important to notice the substantial change of microstructure with the chain length;<sup>29,30</sup> the 1,4-cis content varies between about 42 and 79% in the range of  $\langle M_w \rangle$  between  $9.9 \times 10^3$  and  $1.5 \times 10^6$  g/mol. The vinyl content estimated by <sup>1</sup>H NMR was almost invariable (4–6%) for all of the anionic PB samples prepared at our laboratories.

The change in the microstructure is reflected in the behavior of the glass transition temperatures  $T_g$  given in the fifth column of Table 1, with experimental uncertainty smaller than  $\pm 1$  K. The first two samples in the table have higher  $T_g$ s because of the higher vinyl content relative to the rest of the samples.<sup>1</sup> For the other samples downward in Table 1 there are two factors affecting  $T_g$ : one is the increase of the number average molar mass and the other is the increase in the

cis content. The  $T_g$ s do not reach a limiting value for the high molar mass samples, as would be the case under the action of the first effect only; instead they decrease after having reached a maximum value for  $\langle M_w \rangle$  of the order of  $(1-4) \times 10^5$  g/mol. This behavior is consistent with the microstructure change given in Table 1 and Figure 1. The upturn of the cis-fraction curve in Figure 1 is correlated with a decrease in the glass transition temperature.

**Partial Epoxidation of Polybutadiene.** The names of four ePB samples used as network components and the measured degrees of epoxidation are given in the last two columns of Table 1. The epoxidation degrees as determined by HBr titrimetry<sup>24</sup> were systematically lower than the same as determined by NMR,<sup>15</sup> and the differences are significant relative to the reported uncertainties of the two methods.<sup>15,24,25,31</sup> The discrepancy was probably due to the incomplete titration reaction of the epoxide groups in the two-phase (toluene–acetic acid) titration mixture.<sup>15</sup> The SEC analysis (not shown here) of the ePBs demonstrated that within the analysis' accuracy the epoxidation procedure described in the Experimental Section *does not effect the polydispersity*.<sup>15</sup>

**PB Networks Containing Unattached Chains.** There are two essential conditions to be fulfilled in order to prepare covalently cross-linked networks with molecularly dispersed unattached chains.<sup>2-7</sup> First, the components must be miscible (the *phase problem*), and second, the cross-linking reaction must not affect the unattached chains (the *cross-linking selectivity problem*). The phase problem was studied by DSC measurements of the glass transition temperature<sup>2-5</sup> (see the DSC Measurements subsection). The networks' phase composition is reflected in the rheological measurements, as well, as shown below in the subsection on the rheological characterization. The cross-linking degree and selectivity were studied by swelling and swelling–extraction experiments, respectively (see the next subsection).

**Swelling and Swelling–Extraction Experiments.** The estimated (by swelling experiments in benzene and toluene) number average molar mass per network

Table 2. Thirty Networks with Unattached Chains

sample	net. <sup>a</sup>	$M_{PB} \times 10^{-3b}$	$w_{PB}^c$	mol $e:a:c^d$	$T_g(+20K/min)$ (K)
n1/0	ePB1		0	1:0.36:0.16	188
n2/0	ePB2		0	1:0.33:0.15	183
n3/0	ePB3		0	1:0.50:0.50	187
n4/0	ePB4		0	1:0.35:0.15	180
n4/10/0.10	ePB1	9.90	0.10	1:0.33:0.15	
n4/19/0.10	ePB3	18.6	0.10	1:0.33:0.15	
n4/34/0.10	ePB4	33.6	0.10	1:0.33:0.15	180
n3/50/0.10	ePB3	50.0	0.10	1:0.33:0.15	186
n1/50/0.15	ePB1	50.0	0.15	1:0.33:0.15	185 <sup>d</sup>
n1/50/0.30	ePB1	50.0	0.30	1:0.33:0.15	
n1/50/0.50	ePB1	50.0	0.50	1:0.33:0.15	
n2/50/0.10	ePB4	50.0	0.10	1:0.33:0.15	182
n4/64/0.10	ePB4	64.0	0.10	1:0.33:0.15	
n2/80/0.10	ePB3	80.5	0.10	1:0.33:0.15	
n2/120/0.10	ePB2	120	0.10	1:0.33:0.15	
n4/154/0.10	ePB1	154	0.10	1:0.33:0.15	
n1/235/0.10	ePB1	235	0.10	1:0.36:0.16	
n2/253/0.10	ePB2	253	0.10	1:0.35:0.20	183
n2/253/0.15	ePB2	253	0.15	1:0.35:0.20	183
n2/253/0.30	ePB2	253	0.30	1:0.35:0.20	182 <sup>d</sup>
n2/253/0.50	ePB2	253	0.50	1:0.35:0.20	181 <sup>d</sup>
n4/345/0.10	ePB4	345	0.10	1:0.35:0.15	
n2/430/0.10	ePB2	430	0.10	1:0.35:0.20	183
n1/430/0.15	ePB1	430	0.15	1:0.35:0.20	178; 186
n1/430/0.30	ePB1	430	0.30	1:0.35:0.20	
n1/430/0.50	ePB1	430	0.50	1:0.35:0.20	
n4/550/0.10	ePB4	550	0.10	1:0.35:0.15	
n3/700/0.10	ePB3	700	0.10	1:0.35:0.15	176; 186
n4/900/0.10	ePB4	900	0.10	1:0.35:0.15	180
n4/1500/0.15	ePB4	1500	0.15	1:0.35:0.15	175; 180

<sup>a</sup> Network component from Table 1. <sup>b</sup>  $\langle M_w \rangle \times 10^{-3}$  of PB unattached component from Table 1. <sup>c</sup> Molar ratios of epoxide:anhydride:catalyst. <sup>d</sup> Glass transitions that were broader than those of the pure networks.

strand was  $2700 \pm 500$  g/mol, that corresponds to  $74 \pm 14\%$  efficiency of the cross-linking reaction.<sup>25,34</sup>

The cross-linking selectivity was studied by swelling-extraction tests with a good solvent (benzene) of five networks containing known start fractions of PB10 and PB34. The extracted masses and their distributions were compared with the corresponding quantities before the cross-linking. After the optimization of the cross-linking procedure the extractions were quantitative and the MMDs (SEC traces) of the extracts were indistinguishable from those of the original PBs.<sup>14,15</sup>

The characteristics of 30 networks containing 0–50% unattached PB linear chains are summarized in the Table 2. The names of the networks (first column) are of the form  $nx/y/z$ , where  $n$  stands for *network*,  $x$  specifies the number of ePB (network component) from Table 1,  $y$  specifies the PB unattached component from Table 1, and  $z$  gives the mass fraction of the unattached component. The results from the measurements of the glass transition temperatures  $T_g$  by DSC are listed in the last column and commented on in the next subsection.

**DSC Measurements.** Parts a and b of Figure 2 show the  $T_g$  region of the DSC thermograms obtained with scan rates of  $+20$  °C/min. For clarity, the experimental traces of the networks have been scaled vertically to equal heights. The networks n3/0, n3/50/0.10, and n2/253/0.10 show only one glass transition of similar sharpness. The networks n3/700/0.10 (Figure 2a) and n4/1500/0.15 (Figure 2b) show two glass transitions, one close to the  $T_g$  of the melt and the other one close to that of the pure network (as illustrated in Figure 2a for the case of PB700). Notice that the difference between the two  $T_g$ s of n4/1500/0.15 is of only 5 K. It

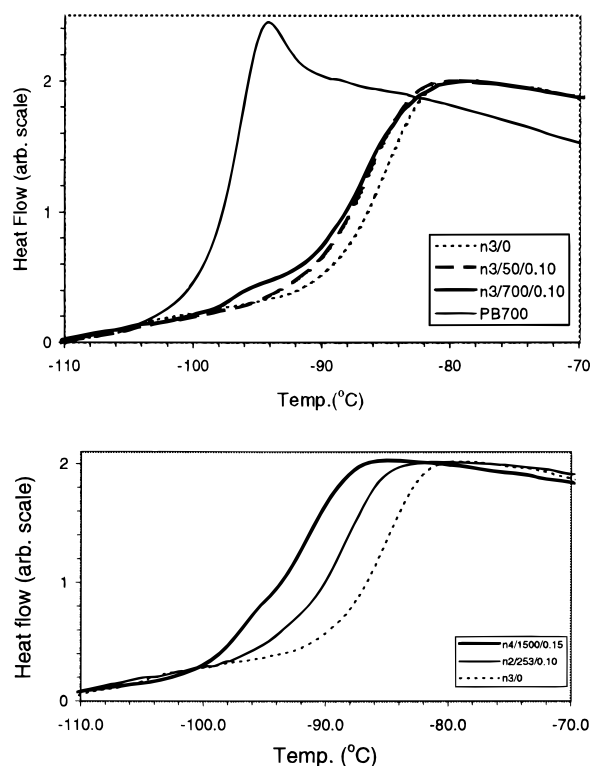


**Figure 2.** DSC thermograms showing the glass transition temperature range for the polymers as listed in the legends: a network with no unattached chains n3/0 (in both a, b (bottom)); a one-phase network with 10% unattached chains n3/50/0.10 (a); a two-phase network with 10% unattached chains n3/700/0.10 (a); one PB melt PB700; another one-phase network with 10% unattached chains n2/253/0.10 (b); and another two-phase network with 15% unattached chains n4/1500/0.15 (b).

was concluded that there is *phase separation* in the cases of n3/700/0.10 and n4/1500/0.15, but possibly not<sup>32,33</sup> in the cases of n3/50/0.10 and n2/253/0.10. The results obtained from the mechanical measurements strengthen this conclusion (see the next subsection on Dynamic-Mechanical Measurements). In the following paragraph we use in advance the strong conclusion, that is, that the samples from the present report showing one single  $T_g$  with transition sharpness similar to that of the “pure” network (see the last column of Table 2) are *one-phase systems*.

The modification of PB by transforming a fraction of the double bonds into more polar epoxide groups changes the interaction between the polymer chains (ePB–PB compared to PB–PB). For the PB-precursor of ePB, which has the *same microstructure* as the PB unattached chains, the most favorable situation for mixing is when the *small concentration* of the epoxide groups is introduced *randomly*<sup>11</sup> in the polymer chains. The DSC trace from n2/253/0.10 (and from other networks with one  $T_g$  value in the last column of Table 2) show a single  $T_g$ , confirming that, within the experimental conditions used in this work, the epoxidation alone does not cause phase separation. For the networks derived from ePB1 and ePB3 of Table 1, there is a sensible difference in the vinyl content between the two components of the network, in addition to the effect of the epoxide groups. This might be the cause of the phase separation observed for the corresponding samples with long unattached chains. Evidently, the phase separation is not observed in the case of n3/50/0.10 containing 10% PB50; this may be because of more similar cis–

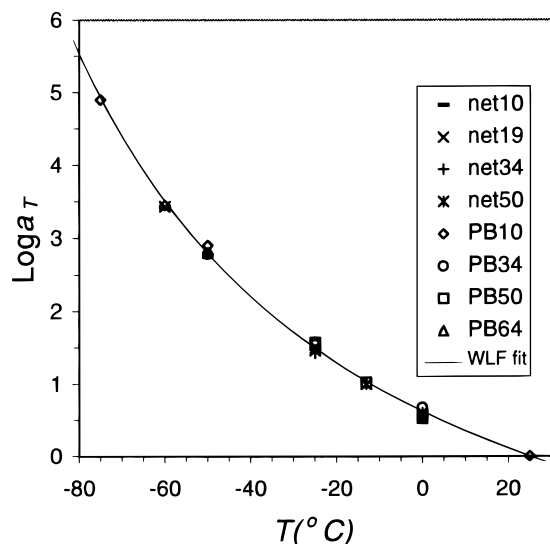


**Figure 3.** Temperature shift factors for PB melts and the respective networks with unattached chains. The solid line is the plot of eq 2.

trans microstructures of the network and the unattached chains and because of the additional free volume introduced by the shorter chains.

The situation is more puzzling for the networks containing more than 10–15% unattached chains (the nuc countersigned with an asterisk in the last column of Table 2). With the experimental conditions and uncertainty given above, the glass transitions of a number of these networks were broader than those of the pure networks, but it was not possible to assign two separate transition temperatures. It will be shown in the section on the dynamic–mechanical measurements that for the series of networks with 30–50% PB253 unattached chains the loss moduli  $G''(\omega)$  ( $\omega$  is the frequency) are broader than the  $G''(\omega)$  of the respective networks containing only 10–15% unattached chains, but the frequency positions of the top of  $G''(\omega)$  have very little difference in the two cases. These findings were interpreted to indicate that the major part of the chains should be in the same phase as the network. With the data at hand it was not possible to go further than these qualitative considerations for this group of networks.

**Dynamic–Mechanical Measurements.** Figure 3 shows the temperature shift factors<sup>1</sup>  $a_T$  for the PB chains in the melts and as unattached chains in the ePB networks. The shift factors were determined by the shift in the frequency scale that produced the best “visual” superposition of the loss moduli  $G''(\omega)$  curves obtained at different temperatures. The measurements were limited to the PB melts with masses of up to 64 000 g/mol (see Table 1) and to the respective nuc (see the plot legend in Figure 3). Within the experimental accuracy the two sets of shift factors are the same. The experimentally determined shift factors were used to reduce to 25 °C the measurements of the dynamic moduli performed at different temperatures by the relations<sup>1</sup>

$$\omega \rightarrow a_T \omega \quad \text{and} \quad G^* \rightarrow G^* T_0 \rho_0 / T \rho \quad \text{with} \quad \rho = \rho_0 + \alpha(T_0 - T) \quad (1)$$

where  $\rho_0$  and  $\rho$  are the densities at the reference temperature  $T_0$  (298 K) and at the measurement temperature  $T$ , respectively;  $G^*$  is the complex modulus<sup>1</sup>

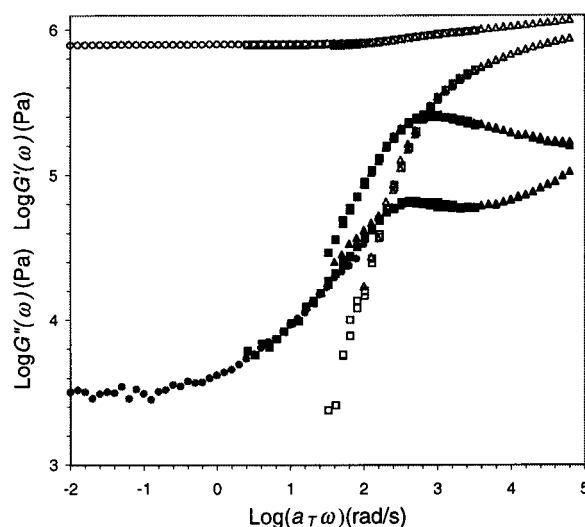


**Figure 4.** Storage moduli  $G'(\omega)$  (empty symbols) and loss moduli  $G''(\omega)$  (filled symbols) reduced at 25 °C for the melt PB34 and the corresponding network n4/34/0.10. Three sets of data obtained at −50, −25, and 25 °C are shown. The temperature shift factors were calculated from eq 2.

and  $\alpha$  is the expansion coefficient at 1 atm pressure. The substituted values were as follows:  $T_0 = 298$  K,  $T = 198, 213, 223, 248, 260, 273$  K;  $\alpha = 7.5 \times 10^{-4} \text{ K}^{-1}$ ;  $\rho_0 \equiv \rho_{298\text{K}} = 0.90 \times 10^3 \text{ kg/m}^3$ . One possible good WLF<sup>1</sup> fit for the data of the melts and the networks (solid line in Figure 3) in the temperature range  $198 \text{ K} < T < 298 \text{ K}$  has the following analytical expression:

$$\log a_T = -3.80(T - 298)/[177 + (T - 298)] \quad (2)$$

which is slightly different from that obtained with data from ref 1 for PB of similar microstructure. The result of data superposition for the cases of PB34 and n4/34/0.10 is shown in Figure 4. The data cover 7 decades in the frequency scale and the superposition is considered satisfactory.

Parts a and b of Figure 5 show the storage moduli  $G'(\omega)$  and the loss moduli  $G''(\omega)$  of the four networks n2/253/10, 15, 30, 50 and the melt PB253. Three comments are considered important relative to Figure 5. First, the loss of the network without unattached chains is much lower than that of the networks with 10–15% unattached chains, which makes the analysis of these last straightforward; that is, the subtraction of the network contribution to the loss modulus does not produce significant changes in the height and form of the  $G''(\omega)$  around the maximum. Second, the form of the  $G''(\omega)$  for the lower fractions of unattached chains is close to the prediction of the reptation theory (this important point is going to be considered in detail in a separate publication<sup>36</sup>). Third, the frequency position of the  $G''_{\text{max}}$  is not very sensitive to the fraction of unattached chains in the range 0.10–0.50; for the sample n2/253/0.10 it is found displaced by a factor of 2.2 toward lower frequencies relative to that of PB253. The narrowing of the  $G''(\omega)$  peak on the high-frequency side for the networks with 10 and 15% unattached chains relative to the  $G''(\omega)$  peak of the melt indicates that there are fewer preterminal relaxation mechanisms in the first case. This is directly related to the longer terminal relaxation time for the unattached chains with respect to the terminal relaxation time of the melt.<sup>36</sup> As anticipated in the preceding subsection, the  $G''(\omega)$

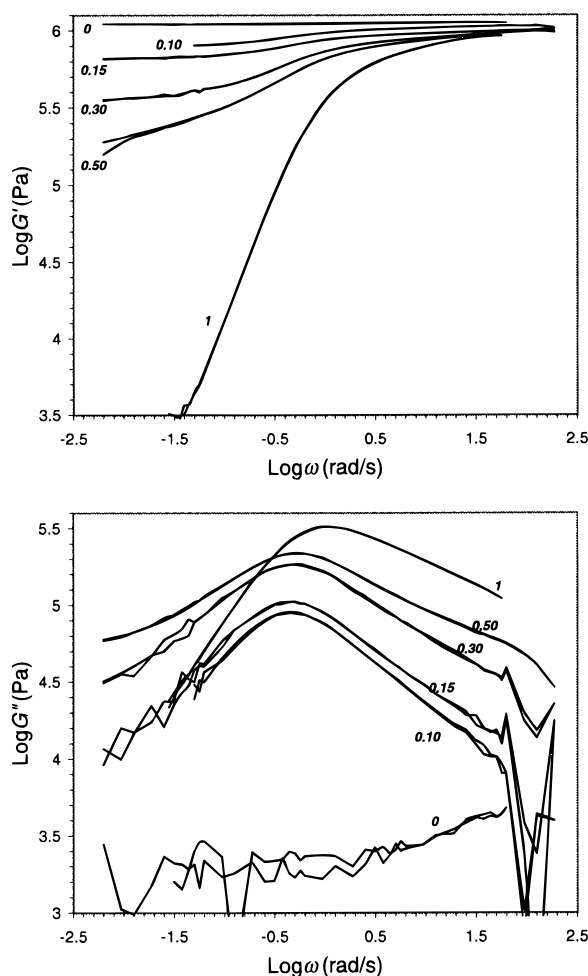


**Figure 5.** Storage moduli  $G'(\omega)$  (a, top) and loss moduli  $G''(\omega)$  (b, bottom) of five networks, n2/0/0, n2/253/0.10, n2/253/0.15, n2/253/0.30, and n2/253/0.50, and one polymer melt, PB253. Double measurements for each sample are shown. See text for discussion.

peaks from the networks containing 30 and 50% PB253 are broader than those of the networks with 10–15% PB253 unattached chains. The analysis of the broadened  $G''(\omega)$  peaks of Figure 5b necessitates additional morphological characterization of the samples and the estimation of the “network background” contribution to the respective  $G''(\omega)$ .<sup>2–6</sup>

The fall in  $G'(\omega)$  from the high- to the low-frequency end in Figure 5a is a measure of the intensity of the relaxation introduced with the unattached chains. If it is assumed that the high-frequency  $G'(\omega)$  (in the rubber plateau zone) is independent of the fraction of unattached chains (this is rather well-supported by the data of Figures 4 and 5a), one can concentrate on the low-frequency level of the storage moduli. The limited set of data from this work for networks with variable concentrations of unattached chains shows that this level is proportional to the 2–3 power of the network component's (ePB) volume fraction (the specific set of data of Figure 5a shows a power 3 dependence). An eventual extension of the experimental work both as a number of samples and as frequency (time) range in the mechanical measurements is a viable possibility for the investigation of the entanglements' contribution to the equilibrium modulus of rubber elasticity.<sup>1,37</sup>

Figure 6 shows plots of the components of the complex modulus for the melt PB1500 and the network n4/1500/

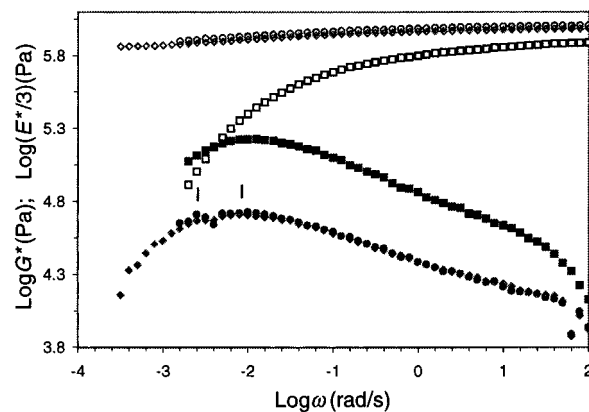


**Figure 6.** Storage moduli  $G'(\omega)$  (empty symbols) and loss moduli  $G''(\omega)$  (filled symbols) of one polymer melt PB1500 (squares) and one two-phase network n4/1500/0.15 (two sets of measurements shown with circles and diamonds). See text for discussion.

**Table 3.** Comparison of the Experimental  $\omega_{\max G''}$  Values and the Reptation Inverse Longest Relaxation Times for the PB Melts and the Unattached Chains in the Networks

sample	$M_w \times 10^{-3}$	exptl $\omega_{\max G''}$ (rad $\times$ s $^{-1}$ )		theoretical $1/\tau_L$ (rad s $^{-1}$ ) <sup>e</sup>	
		melts	networks	$1/\tau_L^{(f)}$ <sup>c</sup>	$1/\tau_L$ <sup>d</sup>
PB10	9.90	67500 <sup>a</sup>	33400 <sup>a</sup>	31600	5860
PB19	18.6		2950 <sup>a</sup>	2580	883
PB34	34.0	740 <sup>a</sup>	360 <sup>a</sup>	301	145
PB50	50.0	220 <sup>a</sup>	100 <sup>a</sup>	81.5	45.4
PB64	64.0	90	40	36.0	21.7
PB81	80.6	38	18	16.9	10.9
PB120	120	12.6	6.0	4.70	3.29
PB154	154	4.0	2.0; 2.0 <sup>b</sup>	2.12	1.56
PB253	253	1.05	0.47	0.446	0.351
PB345	345	0.40	0.20; 0.18 <sup>b</sup>	0.169	0.138
PB430	430	0.14	0.064	0.0856	0.0715
PB550	550	0.090	0.047; 0.035 <sup>b</sup>	0.0400	0.0341
PB900	900	0.016	0.0070; 0.0050 <sup>b</sup>	0.00881	0.00779
PB1500	1500	0.0079	0.0025	0.00185	0.00168

<sup>a</sup> Obtained by using shift factors to values measured at temperatures between  $-75$  and  $0^\circ\text{C}$ . <sup>b</sup> PS–PB block-star thermoplastic networks from ref 14. <sup>c</sup> Inverse of reptation longest relaxation time with contour length fluctuation, eq 5. <sup>d</sup> Simple reptation, eq 4. <sup>e</sup> The calculated values of  $1/\tau_L$  and  $1/\tau_L^{(f)}$  given in ref 14 were by error about 5% higher than the values listed here.

0.15. The measurements of the networks were obtained with the simple elongation geometry; therefore, to compare the results with the shear dynamic–mechanical measurements, the components of the resulting elongation complex modulus  $E^*(\omega)$  were divided by 3.<sup>1</sup> The network is a two-phase system from  $T_g$  measurements (see Figure 2b). It is interesting to notice the bimodal shape of the  $E''(\omega)$  of the network; the main top almost coincides with that of the melt, while the other one is shifted by a factor 3.2 toward lower frequency. This fact was interpreted as following from the existence of the unattached chains both in a separate phase and (a minority of them) as mixed with the network. The top at the lower frequency was taken as representative of the longest relaxation time of the unattached chains in a one-phase system (see Table 3 and Figure 8 below). The bimodality or broadening of the  $G''(\omega)$  top was a general feature of the networks with two  $T_g$ s.

Because of (a) the central importance of the miscibility in the molecular scale of the unattached chains in the discussion of the networks as model systems for testing

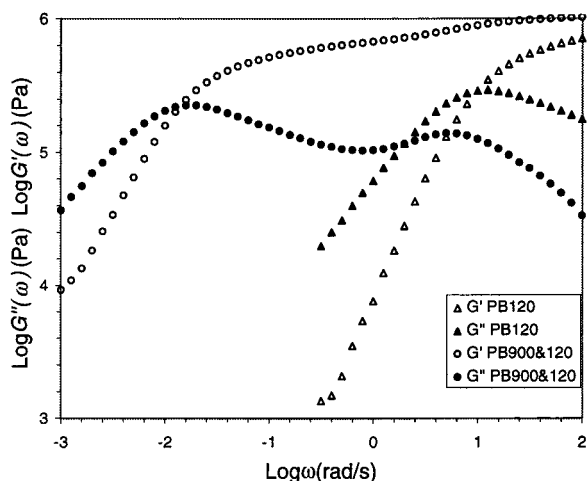


**Figure 7.** Storage (empty symbols) and loss (filled symbols) moduli of PB120 (triangles) and the homogeneous mixture PB900&120 (circles) containing mass fractions of 0.15 PB120 and 0.85 PB900.

the long time dynamics of a chain trapped in a network and (b) the nonconclusive answer given by the  $T_g$  measurements regarding the phase homogeneity,<sup>32,33</sup> another system<sup>11</sup> was prepared.<sup>15</sup> It consisted of mixtures containing about 0.85 mass fractions of a long PB (typically PB900) and 0.15 of a shorter PB (with masses up to 260 000 g/mol). Such mixtures showed one sharp single  $T_g$ , and Figure 7 illustrates the measured dynamic-mechanical  $G^*(\omega)$  for the case of PB900&120. The frequency of the maximum in the loss modulus of the PB120 in the mixture is a factor 2.05 lower than that of the melt PB120. This factor is in good accord with that found for the covalent networks with unattached chains (see ref 15 for more examples). There is little doubt about the one-phase nature of these mixtures.<sup>11</sup> On the basis of this comparison, together with the DSC and the rheology results given above, it was concluded that the networks with unattached chains presented here and showing one single  $T_g$  are *actually one-phase systems*.

**Comparison of the Experimental Data with the Doi-Edwards' Theory.**<sup>12</sup> The dependence of the longest relaxation time  $\tau_L$  on the chain length predicted from the reptation-in-a-tube model was compared with the experimentally measured values from the samples described in the previous (sub)sections. A detailed report on this comparison is found in a separate contribution,<sup>14</sup> and here we summarize the main results (data from four additional samples are presented for the first time here). The frequency of the maximum in the loss moduli  $\omega_{\max G''} \equiv \omega_L$  (rad/s) was connected to  $\tau_L$  by the following simple relation.<sup>14</sup>

$$\omega_L = 1/\tau_L \quad (3)$$

The reptation expression of the inverse longest relaxation time is the following:<sup>12,38</sup>

$$1/\tau_L = (M_e M_0^2 \pi^2 kT)/(b^2 \zeta_0 M^3) \quad (4)$$

and the correction for the contour length fluctuation (superscript (F)) is:<sup>12,39</sup>

$$1/\tau_L^{(F)} = (1/\tau_L)[1 - 1.3(M_e/M)^{1/2}]^{-2} \quad (5)$$

where  $b^2$  is the mean-square end-to-end length per

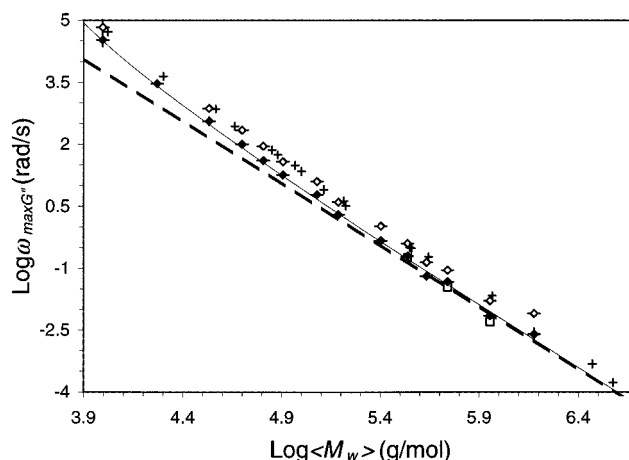


**Figure 8.** Dependence of  $\omega_{\max G''}$  on the  $\langle M_w \rangle$  of PB melts (empty diamonds) and networks (filled diamonds). The crosses are zero shear-rate viscosity data<sup>30</sup> converted by the eq 6. The empty squares are data from the thermoplastic networks of ref 14. The bold dashed line shows  $1/\tau_L$  from eq 4, and the solid line shows  $1/\tau_L^{(F)}$  from eq 5.

monomer unit ( $b = 6.0 \times 10^{-8}$  cm),  $\zeta_0$  is the monomeric friction coefficient<sup>1,12</sup> ( $\zeta_0 = 1.10 \times 10^{-10}$  N s/m),<sup>40</sup>  $M_0$  is the monomer molar mass (54 g/mol), and  $M_e$  is the characteristic entanglement molar mass<sup>1,12</sup> ( $M_e = 1900$  g/mol). All of the values were taken at 25 °C. The results from the oscillatory measurements are summarized in Table 3. Figure 8 compares  $1/\tau_L$  from the Doi-Edwards' theory<sup>12</sup> with the experimental  $\omega_{\max G''}$  from this work. The data points for the unattached chains are shifted toward lower frequencies with factors between 1.9 and 3.2 relative to the data for the respective PB melts. The scaling for both the melts and the chains trapped in networks is  $\omega_L = 1/\tau_L \sim \langle M_w \rangle^{3.35 \pm 0.10}$ , for  $9.9 \times 10^3 \leq \langle M_w \rangle \leq 9.0 \times 10^5$  g/mol (the results from sample PB1500 and the relative network were not included; see the comment at the end of the section on this "anomalous" sample). This result confirms earlier findings. The curve obtained from the reptation model with contour length fluctuation follows well the data for the unattached chains (notice though that the experimental points for the PB900 trapped in a network seem to "continue" under the reptation line; see the comment at the end of section). In the same Figure 8 we show (with crosses) zero shear-rate viscosity ( $\eta_0$ ) data from ref 30 converted by the reptation relation:<sup>38</sup>

$$\eta_0 = (\pi^2/12) G_N^{(0)} \tau_L \quad (6)$$

where  $G_N^{(0)}$  is the rubber plateau modulus<sup>1,12</sup> (1.17 MPa for PB1). These converted data superpose very well with our data, which gives credit to expression 6 as a *quantitative relation* between the zero shear-rate viscosity and the longest relaxation time. The three empty squares stand for data<sup>14</sup> relative to chains trapped in a thermoplastic elastomer network<sup>41</sup> formed by a six arm polystyrene-polybutadiene block copolymer star (PS-PB)<sub>6</sub>. The molar masses of the PS and PB blocks were  $3 \times 10^4$  and  $1.3 \times 10^5$  g/mol, respectively.<sup>14</sup>

Before concluding the present section two additional comments are made with reference to Figure 8. First, notice that the experimental points from our PB with the highest mass (PB1500) do not follow the "general trend". In fact, PB1500 had a rather wide molar mass distribution and a high cis content compared to the other PB samples (see Table 1). The case of sample

PB1500 illustrates the importance of the *mass distribution* and of the differences in *microstructure* on the value of the longest relaxation time. This last effect is also reflected in the apparently lower rubber plateau modulus of PB1500 as compared with that of all the other PB samples, as can be seen from the high-frequency end of the  $G'(\omega)$  in Figure 6. Second, all our data of Figure 8 and the results from previous reports on other chains confined in rubber networks<sup>3–7</sup> strongly indicate that the longest relaxation time of the confined chains are at least a factor 2 larger than the corresponding times of the respective melts. If this is true for “monodisperse” chains with ratios of  $M/M_e$  greater than ours (there is no evident reason for the contrary), one should expect (see, for example, the data points with the highest  $\langle M_w \rangle$  values that continue *under the classical reptation line* (thick dashed line in Figure 8). In other words, one should expect a limiting behavior for the  $\tau_L(M)$  dependence *different from the reptation prediction*.<sup>11,12</sup> In any case, to settle *with confidence* whether the pure reptation prediction is valid<sup>11,12,30,36</sup> or not<sup>42–45</sup> as limiting behavior for very long linear chains requires samples with higher  $\langle M_w \rangle/M_e$  values.

## Conclusions

The preparation for the first time of random polybutadiene (PB) covalent networks containing PB unattached chains was presented. It consists of the slight epoxidation (3–4%) of PB chains and in the selective use of the epoxide groups as cross-linking centers via the reaction of a cyclic carboxyl–anhydride catalyzed by a tertiary amine. The high selectivity of the cross-linking reaction allowed for the formation of the network in the presence of unmodified PB chains; these remain trapped in the network as unattached chains. The described procedure might be easily transferable to other polydienes. The combination of the mentioned procedure with the synthesis of PB by living anionic polymerization allowed preparation of model PB networks containing unattached PB chains. Strong changes in the microstructure (increased 1,4-cis fraction) of PB chains prepared by living anionic polymerization in cyclohexane were observed for masses exceeding  $9 \times 10^5$  g/mol.

The values of the longest relaxation times  $\tau_L(M)$  predicted from the simple reptation model were (for increasing chain length) 12 to 2 times larger than the experimental values of the PB melts. The experimental values of  $\tau_L(M)$  for the chains trapped in the one-phase networks were 1.9–3.2 times larger than the values for the PB melts, and they were closely followed by the prediction of the reptation model corrected with the conjecture of contour length fluctuation. The experimental scaling is  $\tau_L(M) \sim M^{3.35 \pm 0.10}$  (13 samples,  $9.9 \times 10^3 < M < 9.0 \times 10^5$  g/mol) for both the PB melts and the chains trapped in the networks. The larger  $\tau_L$  values for the chains trapped in the networks compared to the  $\tau_L$  of the respective melts have to be related to the narrowing of the  $G'(\omega)$  terminal peak in the first case as compared to the second case.<sup>36</sup>

**Acknowledgment.** We thank Dr. W. B. Pedersen and Mrs. L. Nielsen at the Risø National Laboratory for their kind help with the LALLS measurements. S.N. gratefully acknowledges the financial support by the

Danish Research Academy, Novo Nordisk A/S, Schubert Seals A/S, and The Danish Polymer Center.

## References and Notes

- (1) Ferry, J. D. *Viscoelastic Properties of Polymers*, 3rd ed.; Wiley: New York, 1980.
- (2) Kramer, O.; Greco, R.; Neira, R. A.; Ferry, J. D. *J. Polym. Sci., Polym. Phys. Ed.* **1974**, *12*, 2361.
- (3) Kramer, O.; Greco, R.; Ferry, J. D.; Mc. Donel, E. T. *J. Polym. Sci., Polym. Phys. Ed.* **1975**, *13*, 1675.
- (4) Greco, R.; Taylor, C. R.; Kramer, O.; Ferry, J. D. *J. Polym. Sci., Polym. Phys. Ed.* **1975**, *13*, 1687.
- (5) Nelb, G. W.; Pedersen, S.; Taylor, C. R.; Ferry, J. D. *J. Polym. Sci., Polym. Phys. Ed.* **1980**, *18*, 645.
- (6) Kan, H.-C.; Ferry, J. D.; Fetters, L. J. *Macromolecules* **1980**, *13*, 1571.
- (7) Mark, J. E.; Zhang, Z.-M. *J. Polym. Sci., Polym. Phys. Ed.* **1983**, *21*, 1971–79.
- (8) Barrett, L. W.; Sperling, L. H. *Trends Polym. Sci.* **1993**, *1*, 45–49.
- (9) de Gennes, P. G. *J. Chem. Phys.* **1971**, *55*, 572.
- (10) Edwards, S. F. *Proc. Phys. Soc.* **1967**, *92*, 9.
- (11) de Gennes, P. G. *Scaling Concepts in Polymer Physics*; Cornell University Press: Ithaca, NY, 1979.
- (12) Doi, M.; Edwards, S. F. *The Theory of Polymer Dynamics*; Clarendon Press: Oxford, 1986.
- (13) Ndoni, S.; Vorup, A.; Kramer, O. *Ann. Trans. Nordic Rheol. Soc.* **1993**, *1*, 36.
- (14) Ndoni, S.; Kramer, O. *Europhys. Lett.* **1997**, *39*, 165.
- (15) Ndoni, S. Ph.D. Thesis, University of Copenhagen, 1994.
- (16) Vorup, A. M. Sc. Thesis, University of Copenhagen, 1994.
- (17) Szwarc, M. *Nature* **1956**, *178*, 1168.
- (18) Morton, M. *Anionic Polymerization: Principles and Practice*; Academic Press: New York, 1983.
- (19) Morton, M.; Fetters, L. J. *Rubber Chem. Technol.* **1975**, *48*, 359.
- (20) Ndoni, S.; Papadakis, Ch.; Bates, F.; Almdal, K. *Rev. Sci. Instrum.* **1995**, *66*, 1090.
- (21) Gilman, H.; Haubein, H. A. *J. Am. Chem. Soc.* **1944**, *66*, 1515.
- (22) Gilman, H.; Cartledge, F. K. *J. Organomet. Chem.* **1964**, *2*, 447.
- (23) *Organic Synthesis*; Wiley: New York, 1973; Collect. Vol. 5, p 805.
- (24) Durbetaki, A. J. *Anal. Chem.* **1956**, *28*, 2000.
- (25) Elbek, C. M. Sc. Thesis, University of Copenhagen, 1994.
- (26) Saunders, K. J. *Organic Polymer Chemistry*; Chapman & Hall: London, 1976.
- (27) Worsfold, D. J.; Bywater, S. *Can. J. Chem.* **1960**, *38*, 1891.
- (28) Worsfold, D. J.; Bywater, S. *Macromolecules* **1978**, *11*, 582.
- (29) Ndoni, S. Manuscript in preparation.
- (30) Colby, R. H.; Fetters, L. J.; Graessley, W. W. *Macromolecules* **1987**, *20*, 2226.
- (31) Burfield, D. R.; Lim K.-L.; Law K.-S.; Ng, S. *Polymer* **1984**, *25*, 995.
- (32) Olabisi, O.; Robeson, L. M.; Shaw, M. T. *Polymer–Polymer Miscibility*; Academic Press: New York, 1979.
- (33) Strate, V. G.; Lohse, D. J. *Science and Technology of Rubber*, 2nd ed.; Academic Press: New York, 1994.
- (34) Flory, P. J. *Principles of Polymer Chemistry*; Cornell University Press: Ithaca, NY, 1953.
- (35) Fetters, L. J.; Thomas, E. L. *Mater. Sci. Technol.* **1993**, *12*, 1.
- (36) Ndoni, S. Manuscript in preparation.
- (37) Heinrich, G.; Straube, E.; Helmig, G. *Adv. Polym. Sci.* **1988**, *85*, 33.
- (38) Graessley, W. W. *J. Polym. Sci., Polym. Phys. Ed.* **1980**, *18*, 27.
- (39) Doi, M. *J. Polym. Sci., Polym. Lett.* **1981**, *19*, 265.
- (40) Roovers, J. *Polymer* **1985**, *26*, 1091.
- (41) Bi, L. K.; Fetters, L. J. *Macromolecules* **1975**, *8*, 90; **1976**, *9*, 732.
- (42) Pearson, D. S.; Fetters, L. J.; Graessley, W. W.; Ver Strate, G.; von Meerwall, E. *Macromolecules* **1994**, *27*, 711.
- (43) Deutsch, J. M. *J. Phys. (Paris)* **1987**, *48*, 141.
- (44) Semenov, A. N. *Physica (Amsterdam)* **1991**, *171A*, 517.
- (45) Ndoni, S. *Europhys. Lett.* **1997**, *40*, 219.

MA9714225